https://doi.org/10.5194/acp-2021-87
Preprint. Discussion started: 19 March 2021

Atmospheric Chemistry and Physics Discussions

Morning boundary layer conditions for shallow to deep convective cloud evolution during the dry season in the central Amazon

Alice Henkes[1,4], Gilberto Fisch[1,2], Luiz Augusto Toledo Machado[1,3], and Jean-Pierre Chaboureau[4]

[1]National Institute for Space Research, Cachoeira Paulista, São Paulo, Brazil.
[2]Universidade de Taubaté (UNITAU), Taubaté – São Paulo, Brazil
[3]Multiphase Chemistry Department, Max Planck Institute for Chemistry, Mainz, Germany
[4]Laboratoire d´Aérologie, Université de Toulouse, CNRS, UPS, Toulouse, France

Correspondence: Alice Henkes (alice.henkes@inpe.br)

Abstract. Observations of the boundary layer (BL) processes are analyzed in four shallow convective days (ShCu) and four shallow-to-deep convective days (ShDeep) using a suite of ground-based measurements from the second Intensive Operating Period as part of the Observation and Modeling of the Green Ocean Amazon (IOP2; GoAmazon 2014/5) Experiment. The BL stages in ShDeep days, from the nighttime to the cloudy mixing layer stage, are then described in comparison with ShCu days. Atmosphere thermodynamics and dynamics, environmental profiles, and surface fluxes were employed to compare these two distinct situations for each stage of the BL evolution. Particular attention is given to the morning transition stage, in which the BL changes from stable to unstable conditions in the early morning hours. Results show that the duration of the morning transition on ShDeep days decreases under high humidity and intense vertical wind shear. Higher humidity since nighttime not only contributes to lowering the cloud base during the rapid growth of the BL but also contributes to the balance between radiative cooling and turbulent mixing during nighttime, resulting in large sensible heat flux in the early morning. A large sensible heat flux promotes rapid growth of the well-mixed layer, thus favoring the deeper BL starting from around 08:00 LST. Under these conditions, turbulent mixing provides a lifting mechanism by which air parcels reach the lifting condensation level, leading to the formation of shallow cumulus clouds and their subsequent evolution into deep convective clouds.

1 Introduction

Over land under clear sky and in the absence of any synoptic disturbance, the atmospheric boundary layer (BL) presents a structure that evolves according to a daily cycle of a stable and weakly turbulent at night and an unstable and strongly turbulent during the day (Stull, 1988). The diurnal cycle of the BL processes exerts a strong control on the initiation of convection, especially when mid-and upper-tropospheric forcing is weak (Wilson et al., 1998). BL processes are frequently separated into surface effects, BL effects, and wind circulations (Pielke Sr, 2001). Tightly coupled to the underlying land surface by a strong diurnal cycle of surface fluxes, shallow cumulus clouds can form at the top of the BL. Although generally associated with favorable weather conditions, several factors can potentially dictate whether shallow convection will develop into deep convection, such as free atmospheric moisture, vertical wind shear, cloud aerosol interactions (Chakraborty et al., 2018), and local land-atmosphere interactions (Fitzjarrald et al., 2008).

https://doi.org/10.5194/acp-2021-87
Preprint. Discussion started: 19 March 2021


Atmospheric Chemistry and Physics Discussions

Deep convection clouds are a ubiquitous feature of the atmospheric environment of the Amazon rainforest (Oliveira et al., 2020). During the years 2014 and 2015 in the Central Amazon region, the Observations and Modeling of the Green Ocean Amazon (GoAmazon2014/5 Experiment; Martin et al., 2017) project was carried out to assess the complex interaction between the plume of pollution generated in the city of Manaus-Amazonas, the clouds dynamics and the underlying vegetation (forest and pasture). One of the goals of the project related to the cloud life cycle was to understand physical processes on daily transition in cloud development from shallow to deep convection during wet and dry seasons. Zhuang et al. (2017) using the GoAmazon observations showed the different environmental characteristics and seasonal variations of the transition from shallow to deep convection during the two years of the campaign. The authors found that during the dry season in the central Amazonas, from June to September, a deeper moist layer from the BL to the free troposphere is required for the transition from shallow to deep than during the wet season. Comparing the days with the locally formed daytime deep convective clouds (transition case) with shallow and congestus convective clouds (non-transition), they suggested that in the early morning, between 07:00–09:00 Local Standard Time (LST, the local standard time in Amazonas is UTC-4), the 0–3 km large vertical wind shear (VWS) may appear to link shallow-to-deep cloud conditions during the dry season in contrast to the wet and dry-to-wet transition seasons.

The dry season in the Amazonia is frequently characterized by shallow convective clouds and on some days, there is locally deep moist convection in the early afternoon (Ghate and Kollias, 2016; Tang et al., 2016; Giangrande et al., 2020). The convective regime has a typically bimodal cloud top distribution (Wang et al., 2018), an absence of mid-level clouds, and a shallow-to-deep transition signature (Giangrande et al., 2020). Giangrande et al. (2017) provided a composite analysis of the cloud type frequency collected during the 2-year of GoAmazon campaign. They found that the shallow cumulus clouds represent 22.1% of the total cloud cover, being 16.6% during the dry season and the deep convective clouds account for 5.2%, being 1.5% in the dry season. Despite the lower cloud frequency, the rain rate caused by moist deep convection during the dry season is typically more intense than that of the wet season (Zhuang et al., 2017; Machado et al., 2018).

The role of BL processes and the overlying atmosphere in cloud formation and its transition from shallow to deep clouds remains an important and complex issue in both observational (Zhang and Klein, 2010; Ghate and Kollias, 2016; Tang et al., 2016; Zhuang et al., 2017; Chakraborty et al., 2018; Schiro and Neelin, 2018; Biscaro et al., 2020) and modeling studies where high-resolution models have been used to provide information on the variables that control shallow and deep convection (Chaboureau et al., 2004; Khairoutdinov and Randall, 2006; Wu et al., 2009). Examining the Amazonian BL evolution from night to day has important implications for understanding convection and cloud formation. Indeed, the onset time of a fully convective BL is determined by the surface heat fluxes and the time is taken to eliminate the inversion of the stable BL. Therefore, understanding these complex interactions is a key issue in the description of radiative and hydrological processes as well as the chemical exchange between the forest and the atmosphere.

This study examines the BL processes that influence the convective cloud development, particularly during the dry season when large-scale subsidence is observed that dries out the troposphere and suppresses large scale deep convective clouds. Thus, for the Amazonian BL, we adapt the previous definition of mixed layer growth (Stull, 1988) to a cloudy BL evolution from stable to unstable. The subject of this study considers the evolution of four BL stages until the stage where shallow clouds

https://doi.org/10.5194/acp-2021-87
Preprint. Discussion started: 19 March 2021

Atmospheric Chemistry and Physics Discussions

evolve to deep, as follows: (1) the nocturnal and stable BL stage, (2) the morning transition stage, (3) the rapid growth of the convective BL stage, and (4) the cloudy mixed layer stage. The definition of the BL stages matches with previous studies about morning transition and erosion of nocturnal BL (Angevine et al., 2001; Carneiro et al., 2020; Carneiro and Fisch, 2020), growth of BL (Tennekes, 1973; Stull, 1988; Fisch et al., 2004) and Amazonian cloudy mixing layer (Betts and Viterbo, 2005).

This paper aims to understand the dominant processes in the shallow-to-deep transition during the dry season and to explore the physical mechanisms of the convective cloud-BL interaction. It examines the evolution of the BL structure between nighttime and the fully developed convective stage during four typical shallow cumulus days and four typical shallow-to-deep transition days. For this, we use ground-based observation data at the T3 site (the GoAmazon main site) during the second Intensive Operating Period (IOP2) (Martin et al., 2017) of GoAmazon 2014/5. Although we show in total eight cases studies, the dominant processes are considered to be representative of the typical shallow cumulus and transition from shallow to deep convection as presented by Ghate and Kollias (2016) and Zhuang et al. (2017) during the driest months (e.g. June, July, August, and September) of the GoAmazon 2014/5 campaign.

The article is organized as follows. Section 2 presents the data and the methodology used to identify the cloudy BL stages and to select the convective days. Section 3 describes the environmental conditions and atmospheric stability that are observed by radiosondes. Section 4 presents the surface effects in terms of the daily evolution of meteorological and near-surface variables. Section 5 investigates the atmospheric BL effects on shallow and shallow-to-deep days and the conclusions and next steps are presented in section 6.

2 Data and methodology

2.1 Observations at the T3 site

The T3 site was located at Manacapuru (03° 12’ 36" S; 60° 36’ 00" W; 50 m), 70 km downwind of Manaus, in the central part of the state of Amazonas, Brazil. The vegetation cover at T3 is characterized by pasture site surrounded by forest and nearby the intersection of the Rio Solimões and Rio Negro rivers (Martin et al., 2017). During the GoAmazon 2014/5 campaign, observational data were collected by the Atmospheric Radiation Measurement (ARM) Mobile Facility (AMF-1, Mather and Voyles, 2013).

Meteorological and near-surface variables were measured by five different instruments. The surface air temperature, specific humidity, and wind speed are from the Surface Meteorological system at 1 min time resolution. Average conditional rain rate, which threshold value was greater than 1 mm h^{-1}, is used from the Present Weather Detector at 30 s time resolution. The three wind components, surface sensible and latent heat fluxes are obtained from the Eddy CORrelation Flux (ECOR) (ARM, 2014b) measurement system 3 m above the ground in 30 min averages. Soil moisture (centered at 2.5 cm of depth), and the average soil surface heat flux from the ARM Surface Energy Balance System (ARM, 2014d) at 30 min time resolution. The surface net long-wave and shortwave radiative flux were extracted from the ARM RADFLUX (ARM, 2014c) Value Added Product available at 1 min time resolution.

https://doi.org/10.5194/acp-2021-87
Preprint. Discussion started: 19 March 2021


Atmospheric Chemistry and Physics Discussions

The BL structure was characterized by a laser ceilometer (ARM, 2014a) operating at 905-nm wavelength. The ceilometer retrieves three BL height candidates provided by Vaisala BL-view software at 16 s resolution. The first BL height candidate was used to determine the height during the diurnal evolution of the atmospheric BL in 5 min average. We refer to the BL height alternatively as the BL top or the BL depth associated with the BL mixing layer. The second and third BL candidates were used to estimate the hourly average of residual layer height. To determine the cloud base, the lowest cloud base from ceilometer at 16 s of frequency was used. In addition, the onset of turbulence for the nocturnal BL to morning phase was determined by the vertical wind standard deviation data from the Sonic Detection and Ranging (SODAR) wind profiler (ARM, 2014e) at 30 min time resolution and ranging between 30 m and 400 m.

The environmental condition profile was measured with radiosondes (ARM, 2014f) launched over the T3 site at regular intervals around 01:30, 07:30, 10:30, 13:30, and 19:30 LST during IOP2. Lifting condensation level (LCL), Convective Available Potential Energy (CAPE), and Convective Inhibition (CIN) are computed using sounding data assuming an air parcel in which level of the maximum virtual temperature is in the first 1000 m. Due to the vertical resolution that varies with each launch and the atmospheric conditions, data were linearly interpolated with a resolution of 20 m.

The cloud type profile was from the cloud type product by the ARM Active Remote Sensing of Clouds (ARSCL). The RWP-WACR-ARSCL cloud mask product (Feng and Giangrande, 2018) allows estimating the cloud type profile by combining data from the W-band ARM cloud radar (WACR), radar wind profiler, micropulse lidar, and ceilometer (Giangrande et al., 2017; Feng and Giangrande, 2018). Reflectivity data from the S-band radar, located in Manaus and distant 67.8 km northeast of T3, was used to verify the presence of deep clouds in an area within 60 km of T3.

2.2 The cloudy boundary layer stages

The evolution cloudy BL analysis was divided into four stages according to its daily cycle, the end of each stage corresponding to the beginning of the next stage. Each stage is defined as follows:

(i) Stable stage: The first stage occurs during the nighttime, defined here between 21:00 LST and sunrise (at 06:00 LST).

(ii) Morning transition stage: It is defined as the succession of 3 events: (1) the sunrise, (2) the time when the sensible heat flux becomes positive defined as crossover, and (3) the onset of the convective BL, when the erosion of nocturnal BL is completed and the growth rate of the BL height reaches 100 m h^{-1} (Stull, 1988). The classification of these events follows that proposed by Angevine et al. (2001). This stage during dry season in Amazon region usually occurs two hours after sunrise (Carneiro et al., 2020).

(iii) Rapid growth stage: This stage starts 2 to 3 hours after sunrise, depending on the duration of the morning transition. It ends when the BL height begins to decrease due to the emergence of cumulus clouds. This stage usually occurs between 08:00–09:00 and ends around 11:00 LST.

(iv) Cloudy mixing layer stage: The last stage is between around 11:00 and 15:00 LST. It corresponds to the cloudy mixing layer where a deeper convective BL is observed with cumulus clouds. During this stage that the transition between shallow and deep convection occurs or not.

https://doi.org/10.5194/acp-2021-87
Preprint. Discussion started: 19 March 2021

Atmospheric Chemistry and Physics Discussions

2.3 Selection of shallow convective and shallow-to-deep convective days

The shallow and shallow-to-deep convective days were searched in the dry season during the IOP2 (from 15 August to 15 October 2014; Martin et al., 2016; Giangrande et al., 2017). This selection period was limited to the period from 22 August to 15 October, when an additional radiosonde was launched at 10:30 LST to enhance the diurnal radiosonde coverage. The period from 13 to 29 September was excluded from the analysis as no WACR radar data was available. October days during the IOP2 were not considered since October is considered a dry-to-wet transition season. Cloud-type definitions based on cloud boundaries and thickness are from Giangrande et al. (2017) and the criteria to characterize shallow and shallow-to-deep convective days are adapted from Zhang and Klein (2010) and from Zhuang et al. (2017) and it is defined as follows:

Shallow convective days (ShCu): They are defined as days with shallow cumulus in late morning or early afternoon observed by the ARSCL product. The cloud top height is under 3 km, and the cloud base height is around 2 km. In the region within a radius of 60 km of the T3 site, the reflectivity of the S-band radar is less than 20 dBz, at all hours of the day suggesting that there is no deep convection influence on the T3 site. No precipitation is measured at any time of the day.

Shallow-to-deep convective days (ShDeep): They are characterized by shallow cumulus clouds observed during the growth of the convective layer stage, with cloud base within the BL (around 1-2 km depth) and rising gradually over time until convective development from shallow to deep. Unlike ShCu days, the transition from shallow-to-deep cloud cover is observed by the ARSCL product. The deep convective cloud is characterized by a base under 3 km, a top above 3 km, and a thickness greater than or equal to 5 km. Precipitation occurs during the cloudy mixing layer stage and is higher than 1 mm h^{-1}.

From 22 August to 13 September 2014, following the criteria defined above, a total of 5 shallow cases with deep convection around T3 (but not above), 2 cases of deep convection during the night, 7 shallow to congestus cases, and 4 ShCu days and 4 ShDeep days were identified. Among them, only the 4 ShCu day and ShDeep days were selected. On the ShDeep days, the triggering from shallow-to-deep convection occurred at different times in the afternoon (Fig. 1), which were observed between 12:00 and 16:00 LST. During the nights preceding the events, these selected days do not show deep convective clouds but generally a few cirrus clouds above 8 km. The dates and the list of relevant features are given in Table 1. Figure 1 shows the cloud-type classification from the merged RWP-WACR-ARSCL on each ShCu and ShDeep day.

3 Environmental conditions and atmospheric stability

The soundings are used to investigate environmental conditions and atmospheric stability as well as their diurnal variation with the convection cycle. Figure 2 shows the vertical profile for relative humidity (RH), potential temperature, specific humidity, and wind speed measured by radiosonde on ShDeep and ShCu days. The launch times allowed allocating the radiosondes profiles to the stages, as follows: the stable stage at 1:30 LST, the morning transition stage at 7:30 LST, the rapid growth stage at 10:30 LST, and the cloudy mixing layer stage at 13:30 LST. The differences between ShDeep and ShCu days are compared by the mean (red and blue lines) and its standard deviation (shaded region) in the lowest 3500 m.

Comparing the RH profiles between ShDeep and ShCu days, there is a significant difference of moisture in the vertical profile of RH on ShDeep days (Fig. 2a). Not only is the humidity higher on ShDeep days, but it is almost constantly distributed

https://doi.org/10.5194/acp-2021-87
Preprint. Discussion started: 19 March 2021

Atmospheric Chemistry and Physics Discussions

along the vertical direction. At all stages, the RH is 10 % higher on ShDeep days in the layer beneath 2000 m than on ShCu days. Above 2000 m, the differences between ShDeep and ShCu are even more important. On average, the RH on ShDeep days are 40 % higher than ShCu days during the stable stage and morning transition and up to 50 % during the rapid growth stage and cloudy mixing layer stage. This reflects the importance of mid-level humidity during the dry season as observed by Ghate and Kollias (2016); Zhuang et al. (2017), and Chakraborty et al. (2018).

The potential temperature profiles are shown in Fig. 2b. A weakly stable layer is found at 01:30 LST for both convective regimes. The potential temperature near the surface increases, from the night to morning by about 1.0 K on ShDeep days while on ShCu days the changes are about 0.3 K. At the morning stage (07:30 LST), a shallow mixed layer capped by a stable BL inversion above is observed due to the evolution of the convective layer. At 10:30 LST, there are well-mixed layer conditions during the rapid growth stage for both convective regimes. At 13:30 LST, there is not well-defined mixed layer on ShDeep convection days due to the effects of precipitation while a deepened well-mixed layer is found on ShCu days. From the stable, the morning transition, to the rapid growth stages on ShDeep days, the potential temperature profile is slightly cooler (about 1.0 K) than on ShCu days in the layer under 1000 m. In the cloudy mixing layer stage (13:30 LST), the colder low atmosphere during ShDeep days is also associated with precipitation caused by downdrafts, which may occur during the ascent period of the sounding on the subcloud layer.

The vertical distribution of water vapor is higher on ShDeep days than on ShCu days from the stable stage (01:30 LST) to the morning transition stage (07:30 LST) as well as during the daytime stages 10:30-13:30 LST (Fig. 2c). More specifically, the temporal evolution of specific moisture profiles clearly show that ShDeep days are moister (by 2.0 g kg^{-1}) than ShCu days. The layer above BL from stable stage to morning transition stage also differs on ShDeep and ShCu days. For instance, on the ShDeep day profiles, the specific humidity is higher by about $\sim$0.5 g kg^{-1} at $\sim$ 1200 m, while on ShCu days, it is lower by about -1.0 g kg^{-1}. During the rapid growth stage, there is a difference of about 2.0 g kg^{-1} under 3000 m. During the cloudy mixing layer stage, there is a difference of about 3.0 g kg^{-1} beneath 1000 m, and above this level there is a decrease with height.

The wind speed increases with the height, from the surface to 3000 m, except in the 07:30 LST sounding (Fig. 2d). The wind speed profiles show an overlap of large standard deviation in both convective regimes. These large standard deviations indicate high variability in the vertical wind speed profiles. The difference in horizontal winds between the two convective regimes is found during the morning transition stage (07:30 LST sounding). On ShDeep days, there is a maximum value of 12 m s^{-1} at a height $\sim$ 1200 m. On ShCu days, the maximum wind value is approximately 10 m s^{-1} at an altitude of 500 m. The contrast between the vertical variation of the wind suggests a larger wind shear on ShDeep days. These features were also found by Zhuang et al. (2017), in which the 0-3000 m bulk vertical wind shear reaches a maximum of about 9 m s^{-1} during the morning transition in the dry season considering the two years of the GoAmazon campaign (see Fig. 14 in Zhuang et al. (2017)). As a consequence, these larger values of vertical wind shear on ShDeep days might provide an elevated source of turbulent mixing (Mahrt and Vickers, 2002) during the morning transition that influences the growth of the convective BL.

The difference observed in the potential temperature and specific humidity profiles suggest that both the profiles observed below 1000 m and the higher specific humidity content in the BL and lower free troposphere contribute to higher RH profiles

https://doi.org/10.5194/acp-2021-87
Preprint. Discussion started: 19 March 2021


Atmospheric Chemistry and Physics Discussions

on ShDeep days. Temporal variations in temperature and moisture observed in the BL and lower free troposphere also resulted in considerable differences in convective indices. Figure 3 shows the evolution of the mean and standard deviation of the LCL, CIN and CAPE. Closely associated with high specific humidity values on ShDeep days produces a lower LCL and CIN. On ShDeep days, the lower LCL associated with rapid formation of convective BL results in an overlap of these two zones and cumulus formation earlier in the day. CAPE values are high for both ShDeep and ShCu days, and in particular, its maximum is observed around 10:30 LST the nearest time before the triggering of deep convection (e.g., Zhuang et al., 2017). The increase in humidity at low and mid-levels contributes to the change in atmospheric stability and thus to the triggering of the transition from shallow to deep convection. This result agrees with the findings of several related studies on the evolution of deep moist convection in the dry season during GOAmazon 2014/5 (Ghate and Kollias, 2016; Zhuang et al., 2017; Chakraborty et al., 2018).

4 Surface effects

4.1 Net radiative, soil moisture, and turbulent heat fluxes at the surface

Figure 4 shows evidence of the cloud responses to surface effects and vice versa. The net shortwave radiative flux during the night is zero and, after sunrise, it increases to a maximum of $\sim$ 800 W m^{-2} at noon, and decreases in the afternoon (Fig. 4a). It is modulated by the diurnal development of convective clouds. During the rapid growth stage, the main differences between ShDeep and ShCu days occur in the late morning due to the shallow cumulus cloud cover, and in the early afternoon, when convective storms produce precipitation that reduces shortwave solar radiation at the surface. This results in radiative cooling at the surface during ShDeep days compared to ShCu days during the morning or afternoon. On ShDeep days, the net shortwave is lower than on ShCu days by an average of 70 W m^{-2} between 09:00 and 10:00 LST, and 200 W m^{-2} between 12:30 and 15:00 LST. The net longwave flux at the surface is always negative (Fig. 4b). The more negative the values are on ShCu days, the higher the outgoing longwave radiation is compared to ShDeep days. The difference between ShDeep and ShCu days is around -10 W m^{-2} during the stable stage and increases during the day as the cloud fraction. The higher humidity profile in ShDeep days is probably the reason for this difference.

Soil moisture is an important factor because it controls the partitioning of the available energy between the surface latent and sensible heat fluxes. The mean soil moisture is lower on ShDeep days than on ShCu days in the superficial layer at 2.5 cm (Fig. 4c). In particular, there is a large overlap in standard deviation suggesting that there are days when the percentage of soil moisture is similar between the two convective regimes due to day-to-day variations. Since we found differences in the longwave radiative flux and soil moisture between ShDeep and ShCu days, differences in soil heat flux between convective regimes are expected. This is shown in Fig. 4c, which represents the time evolution of the average soil surface heat flux for the soil layer $0-5$ cm. For the stable stage, the soil heat flux is positive (directed into the soil). On ShDeep days, the soil absorbs less energy than on ShCu days during nighttime. The morning transition stage is characterized by a crossover of the signal (positive to negative) around 8:00 LST in the morning in both convective regimes. The soil heat flux reaches a maximum of about -35 Wm^{-2} around noon indicating an amount of released energy directed into the atmosphere. In the cloudy mixing

https://doi.org/10.5194/acp-2021-87
Preprint. Discussion started: 19 March 2021


Atmospheric Chemistry and Physics Discussions

layer stage, the corresponding negative values and the large standard deviation on ShDeep days are associated with cooling by rain and the soil heat flux changes its flow direction around 16:00 LST. On ShCu days, the evening crossover occurs after sunset.

The time evolution of the surface fluxes is in phase with the shortwave radiation (Fig. 4a). The surface latent heat flux reaches a maximum of 290 W m^{-2} on ShDeep days and 310 W m^{-2} on ShCu days (Fig. 4c). On ShDeep days, the latent heat flux is lower than on ShCu days from 09:00 LST to 17:00 LST. This difference could be due to the early deepening of the BL, redistributing water vapor in the BL depth. The reduction of latent heat flux on ShDeep days is similar to that found over to the U.S. Southern Great Plains (SGP) site shown by Zhang and Klein (2010). At nighttime, due to surface longwave radiative cooling, the surface sensible heat is near zero or eventually slightly negative for both ShDeep and ShCu days (Fig. 4d). Early in the morning, the difference between ShDeep and ShCu days becomes significant after 07:00 LST, when the surface leads to an upward exchange of sensible heat and subsequent warming of the lowest part of BL due to heat flux convergence. During the morning transition stage, the sensible heat flux reaches mean values 20 W m^{-2} greater on ShDeep days than on ShCu days. In the rapid growth stage, around 10:00 and 11:00 LST, the average sensible heat flux on ShDeep days reaches a peak of 50 W m^{-2} higher than on ShCu days. The peak corresponds to the time before the triggering of deep convection. As expected, a drastic decrease of the surface heat flux is observed during precipitation events, around 13:00 LST with a decrease of almost $\sim$ 30 W m^{-2} and around 16-17:00 LST with a decrease of $\sim$ 70 W m^{-2}.

We find larger average sensible heat flux and smaller average soil moisture on ShDeep days. However, we did not see strong differences in latent heat flux at surface. Changes in the energy partition influence the heat flux within the BL resulting in inhomogeneity in this layer and affecting its atmospheric stability, thus increasing the potential for convective cloud formation on ShDeep days.

4.2 Surface inhomogeneity

The convective BL growth is forced by turbulent surface heat fluxes, which are controlled by instability and surface heterogeneity effects. Figure 5 shows the time evolution of the average air temperature at 2 m, specific humidity at 2 m, horizontal wind speed, and turbulent kinetic energy (TKE) and their standard deviation. The air temperature gradually decreases from 20:00–06:00 LST, with rates of 1.1°C and 2.3°C on ShDeep and ShCu nights, respectively. During the stable stage, the near surface air temperature is controlled by longwave radiative cooling (Fig. 4b) and turbulent mixing. In the predawn hours, ShDeep days have higher surface temperatures on average (by about 0.5 °C) between 04:00 and 06:00 LST, unlike ShCu days. Followed the morning part of the air temperature evolution, which includes the morning transition stage and the rapid growth stage, there is an intense gradual warming of 8.0°C on ShDeep days and 10.0°C on ShCu days until the diurnal cycle reaches the maximum air temperature around noon. Later, on ShDeep days, after the air temperature reaches the maximum of 33.0°C around 12:00 LST, a drop of $\sim$3.0°C is observed due to the latent cooling from rain evaporation. On ShCu days, during the cloudy mixing layer stage, the air temperature decreases after the maximum of 34.5°C around 15:00 LST.

Figure 5b shows the time evolution of the specific humidity, with similar behavior of air temperature. The specific humidity gradually decreases during the stable stage of the BL. For ShDeep days, the range is smaller than for ShCu days with rate

https://doi.org/10.5194/acp-2021-87
Preprint. Discussion started: 19 March 2021


Atmospheric Chemistry and Physics Discussions

values of 1.1 g kg^{-1} during ShDeep nights compared to 2.0 g kg^{-1} in ShCu nights in 8 h. By ∼06:30 LST, the specific humidity is minimum followed by an increase of almost 3.0 g kg^{-1} of moisture at 08:00 LST. After 09:00 LST, the specific humidity on ShDeep days decreases slightly in the afternoon on the order of −1.0 g kg^{-1} between 12:00–16:00 LST at the time of precipitation. This drying of the BL on ShDeep days suggests that downdrafts are not able to bring air down from a high enough altitude to produce significant surface drying as it occurs in some cases of isolated convection (Oliveira et al., 2020) and also organized systems with system passages (Schiro and Neelin, 2018). While on ShCu days, the specific humidity decreases around 2.0 g kg^{-1} until the sunrise, followed by a later maximum at 19:00 LST.

In order to characterize the dynamical aspects of BL inhomogeneity, Fig. 5(c-d) shows the horizontal wind speed and turbulence intensity, which was checked by means of TKE. TKE is calculated as half of the sum of the variances of the wind components (TKE $= 0.5\sqrt{\overline{u'^2} + \overline{v'^2} + \overline{w'^2}}$). On ShDeep days, the mean nighttime surface wind speed is slightly larger than on ShCu days. For instance, from 22:00 to 02:00 LST, the period shows signs of intermittent turbulence, with winds becoming stronger (around of 1.5 m s^{-1}) and TKE peaks of ∼0.3 m^2 s^{-2}, as expected since stronger winds imply increased mechanical production of turbulence at nighttime. Since the beginning of the convection, the daytime surface wind and the TKE increase. The TKE difference can be distinguish between the convective regimes during and after the passage of convective storms. Substantial enhancements of TKE are observed of about 1.5 m^2 s^{-2} at 13:00 LST and about 0.5 m^2 s^{-2} at 15:00 and 16:00 LST. These transient peaks of TKE are probably associated with convective storm downdrafts at the time the gust fronts arrived at the T3 site (Oliveira et al., 2020).

5 Boundary layer effects

5.1 Comparing the boundary layer evolution between ShDeep and ShCu days

The daily evolution of the BL height is analyzed in Fig. 6 for ShDeep and ShCu days. It shows typical characteristics of the known Amazonian BL (Carneiro and Fisch, 2020), with minimum heights during nighttime and maximum around noon (Fig. 6, lines). During the night, the BL is established as an intermittent weakly stable layer, in which the BL depth decreases gradually from 20:00 LST to sunrise, ranging from 400 to 140 m on ShDeep days, and from 300 to 110 m on ShCu days. The average depth of the stable layer is higher on ShDeep days than on ShCu days (by about 80 ± 50 m over the whole stable stage). The relatively higher values of nocturnal BL height are related to more turbulent mechanical mixing on the stable stage on ShDeep days than on ShCu days, as shown in Fig. 5d.

The morning transition stage begins at sunrise and is determined by the time when the surface heat changes from negative to positive values, that is ∼07:00 LST (Fig. 4d). When the surface warms around 07:00 LST on ShDeep days, there is a slight increase in the BL depth. This stage ends around 08:00 LST, at which time the net radiation is ∼240 W m^{-2} and the sensible heat flux is about 39 W m^{-2}. Moreover, on ShCu days, the BL depth grows slowly from the approximately same time and ends 0.75 h later (around 08:45 LST), at which time the net radiation is ∼290 W m^{-2} and the sensible heat flux is about 42 W m^{-2}. During this transition stage, the stable BL inversion is completed eroded and replaced with a convective BL. A noticeable

https://doi.org/10.5194/acp-2021-87
Preprint. Discussion started: 19 March 2021


Atmospheric Chemistry and Physics Discussions

difference between the convective regimes is that the period of the morning transition is shorter for ShDeep days than for ShCu days.

Throughout the rapid growth stage, the BL height advances rapidly through the morning. On ShDeep days, the beginning is observed 2 h after sunrise (end of morning transition stage) with a BL height of about ∼300 m and to continue to a height of ∼2000 m reaching through the residual layer around 09:30–10:00 LST (Fig. 6, dashed lines). During ShCu days, the BL takes 3 h after sunrise to extend from ∼300 m through the residual layer (around 2000 m). By the time the residual layer from the previous day is incorporated into the rapid growth, there is an increase in the buoyancy entrainment flux probably due to the moist low-troposphere (between surface and 1500 m) (Chakraborty et al., 2018) which leads to a well-mixed layer supporting the formation of the deeper cloudy BL, on both convective regimes. ShDeep days reach a maximum height (in the mean) of ∼ 2100 m around 10:00 LST and then decrease in height during the emergence of shallow formation and during its growth into a deep cloud. ShCu days reach a maximum height (on average) of ∼ 2250 m around 13:00 LST and then decay in height in the late afternoon due to decreasing surface fluxes (Fig. 4e-f).

5.2 The morning transition boundary layer and its relation to the afternoon ShDeep convection

Many processes influence the BL throughout the diurnal cycle, such as surface heating, entrainment at the BL top, direct radiative heating or cooling of the air, and cloud effects (Angevine et al., 2020). Here, the dependence of meteorological parameters and processes on the BL associated with a more rapid transition to the convective onset is shown for each ShDeep and ShCu event. As noted previously, the response of the convective regimes depend on the tropospheric state, more specifically on the integrated-column humidity, and on the BL processes. On ShDeep days, the nocturnal BL evolution during the stable stage is characterized by more mixing and less time to erode the stable BL inversion, leading to an early well-mixed layer that favors the rapid formation of the convective BL compared to ShCu days. During the morning transition stage, humidity and VWS can be relatively large in the 1000 m layer as well as the sensible heat flux at the surface. This suggests that some of the warming that is eroding the stable BL may be associated with surface and top-down effects, similar to previous findings on the morning transition (e.g. Angevine et al., 2001, 2020).

The main characteristics of the morning transition of all days are given in Table 2 (a variation of this table can also be found in Fig. 7). It is shown the crossover time and the time of the first significant positive values of the sensible heat flux, the onset of the convective BL (CBL) that refer to the time necessary with respect to sunrise to complete eroded the stable BL which the end of morning transition stage is taken as onset of convective BL. The integrated water vapor (IWV) is calculated in the column from 50 to 1000 m (IWV_{1km}), and in the total vertical column, from 50 to 20000 m (IWV_T), and are shown in brackets (Table 2). The vertical wind shear (VWS) is calculated by subtracting the mean horizontal wind speed at 1000 m from the mean 50 m wind speed at 7:30 LST radiosonde profile. Days with cloud influence during the morning-transition stage are marked with an asterisk in the table. Angevine et al. (2001) has shown that the most extreme day-to-day variations in the duration of the morning transition were found on days with cloud influence at Cabauw tower in the Netherlands. The daytime convective BL over Amazonia is generally cloud influenced and rarely cloud-free (Betts et al., 2009), therefore days with cloud influence during the morning transition stage are not excluded from the analysis.

https://doi.org/10.5194/acp-2021-87
Preprint. Discussion started: 19 March 2021


Atmospheric Chemistry and Physics Discussions

On average, the duration of the morning transition stage for the four ShCu days is about 2.5–3.0 h after sunrise and the specific humidity decreases sharply from $\sim$ 19 to 12 g kg^{-1} for the layer between 50 and 1000 m. Among ShCu days, day 1 (25 August) and day 4 (4 September) are cloud-free days. The time required for the sensible heat flux to cross over zero is 1.5 h and the onset of the convective BL is observed about 2.5 h after sunrise for both days. These two days have respectively the greatest and the smallest height rate-of-change among ShCu days. The height rate-of-change is 84 m h^{-1} for day 1 and 43 m h^{-1} for day 5. The difference between these days is probably due to the larger sensible heat flux at the time of the crossover and the vertical structure of the specific humidity as well as the IWV$_T$ of 4.6 cm for day 1 compared to 3.6 cm for day 4. The days moderate the VWS by 5.1–4.8 m s^{-1}. For both ShCu days with cloud influence, day 3 (3 September) has the earliest crossover among ShCu days of around 0.5 h after sunrise, and has the last CBL onset at 09:00 LST, 3.0 h after sunrise probably due the shallow cumulus cover observed between 07:00 and 08:00 LST. Day 5 (5 September) has a low height rate-of-change (56 m s^{-1}) and the smallest VWS of all days (3.2 m s^{-1}). The crossover occurs at 1 h after sunrise and the onset is 2.5 h after sunrise.

Based on the ShDeep days, low cloud cover is present on 3 of the 4 days. The average duration of the transition is about 2.0 h for the cloud-free day and days with shallow cloud influence. On ShDeep day with shallow and altocumulus cloud influence during the whole morning transition stage, the duration is about 2.5 h. In all ShDeep days, the specific humidity decreases from $\sim$20 to $\sim$ 15 g kg^{-1} for the layer between 50 and 1000 m. On day 2 (27 August), shallow cumulus and altocumulus are reported before and after sunrise, however, the sunrise follows the crossover by 0.5 h and after that, between the crossover and the onset, there has no influence of clouds and the onset of convective BL is approximately 2.25 h after sunrise. For the day 3 (7 September), shallow clouds are observed between 06:00 and 07:30 LST, the crossover is 1.0 h (07:00 LST) after sunrise and the onset follows at around 08:10 LST. Day 7 also has a high BL height rate-of-change like day 2 and day 6 of about 200 m s^{-1}. However, the onset of convective BL is delayed by 2.5 h after sunrise probably due to altocumulus and cumulus cover during the transition. The last selected ShDeep day is 12 September, the only cloud-free morning and the smallest BL height rate-of-change and VWS among ShDeep days. The sensible heat flux crossover time is 06:30 LST and the onset occurs 2 h after sunrise (08:00 LST).

The early onset of the convective BL is visible on ShDeep days as a clear increase in turbulence (about 0.1 $\mathrm{m\,s^{-1}}$) in the standard deviation of the vertical wind speed contour (Fig. 8). Thus, there is a good agreement of the early onset observed by the ceilometer on ShDeep days (Fig. 8e-h). Furthermore, the SODAR profile onset time is a little later on ShCu days (Fig. 8a–c) as observed by the ceilometer.

After detecting the large VWS in the morning transition sounding, we found that the VWS above the BL is generally associated with the occurrence of low-level jet (LLJ) stream in 7 of the 8 days (Table 2). The exception is day 8 on 12 September, which shows a VWS of 7 $\mathrm{m\,s^{-1}}$. The LLJ is observed as a low-level maximum speed in the vertical wind profile, in which the wind is faster than the wind speeds above and below it in the lowest 1500 m of the atmosphere (Stull, 1988). On ShDeep days, the maximum wind speed is 10–12 $\mathrm{m\,s^{-1}}$ located between 630 and 1350 m above the ground. On ShCu days, the wind speed profile indicates the development of a LLJ with the nose (maximum wind speed) of the jet located at a height

https://doi.org/10.5194/acp-2021-87
Preprint. Discussion started: 19 March 2021


Atmospheric Chemistry and Physics Discussions

of around 350–630 m, with a maximum speed of about 6–15 $\mathrm{m\,s^{-1}}$. The deeper LLJ on ShDeep days may be associated with large-scale moisture advection above the BL as showed by Ghate and Kollias (2016).

The scatterplots in Fig. 9 show the relation between morning transition BL height rates-of-change and (a) IWV_{1km} and (b) VWS between 50 m and 1000 m, respectively. The BL height increases with time due to the surface heating. This rate-of-change, during the transition from night to morning, indicates a positive association of a high rate-of-change of the BL height due to the high values of IWV_{1km} and VWS (i.e, the duration of the morning transition on days with ShDeep convection decrease at high humidity content and at intense VWS in the early morning, both for cloud-free and cloudy-influenced mornings).

6 Conclusions

This study presents an observational analysis of atmospheric BL processes from the nighttime stable stage to the cloudy developed stage during the dry period over Manacapuru, Amazonas, Brazil. The data used here were collected at T3 site during the second Intensive Operating Period (IOP2) in the Green Ocean Amazon 2014/5 (GoAmazon) field campaign. These data are used to study four shallow convective days (ShCu) and four shallow-to-deep convective days (ShDeep). Average BL height cycles consist of distinct phases of evolution from a clear to a cloudy BL, which are referred to as the stages of a cloudy BL. The main findings are summarized in the conceptual schematic shown in Fig. 10.

The environmental conditions (i.e., in the lower free troposphere) in which the BL grows during ShDeep days are relatively moister and colder than in the environmental conditions in which ShCu days are observed. Analysis of the vertical structure of wind speed shows that VWS is generally associated with the occurrence of maximum wind speed (i.e., low-level jet). ShDeep days are associated with larger wind shear and wind maximum in the upper layer between 630–1350 m. ShCu days are associated with moderate VWS and wind maximum in the lower layer between 350–630 m.

The evolution of the ShDeep stable stage is characterized by the balance between radiative cooling and turbulent mixing, with higher humidity and near-surface air temperature being observed, unlike the ShCu stable stage. Its mean BL depths in the convective regime decreases gradually from 20:00 LST to sunrise, ranging from 400 to 140 m on ShDeep days, and from 300 to 110 m on ShCu days.

Due to the different nighttime and environment conditions, the most marked variations in the BL stages are in the morning transition stage. The duration of the morning transition stage on ShDeep days decreases when humidity is high and VWS is intense in the early morning hours. This rapid transition to convective onset can be attributed to a combination of variables before sunrise, 2 m specific moisture, such as warm air temperature controlled by radiative cooling and turbulent mixing, and surface wetness. Collectively, the early erosion and early peak of the growth stage respond to changes in the partitioning between surface heat fluxes by increasing the surface sensible heat flux and lowering the LCL in the early morning, suggesting that the surface heat flux will force the growth of BL. Specifically, the humidity and wind shear from above have a significant effect in accelerating the vertical mixing motion. This suggests that the morning transition of the nocturnal BL does play a role

https://doi.org/10.5194/acp-2021-87
Preprint. Discussion started: 19 March 2021


Atmospheric Chemistry and Physics Discussions

in the vertical motion during ShDeep days. In consequence, the onset of full convection (e.g, well-mixed layer) at the end of the morning transition stage occurs early.

In terms of cloud cover on the morning transition stage, scattered shallow clouds do not seem to directly influence the development of convection on ShDeep days. It is only when there is more cloud cover, such as altocumulus and shallow cumulus, during the whole stage that a delay is observed at the onset of the convective BL (i.e., event 7). However, shallow cumulus cover appears to delay the morning transition from the crossover to the onset of the convective BL during ShCu days.

During the rapid growth stage, vertical mixing in the deeper BL will entrain moist air into the BL through which the air parcel can reach the LCL (thus causing the first cell of shallow cumulus to emerge) and then the level of free convection (thus favoring deep convection).

The analyses of diurnal cycle of ShDeep and ShCu days show that the wet and sheared environment is at the origin of the main modifications of the BL since nighttime and early morning stages. It should be noted that four-day ShCu and four-day ShDeep averages are incomplete to fully understand the seasonal behavior in the cloudy BL varying each day during the dry season. However, these individual days show a wide range of behaviors, dominated by environmental conditions, in which several days can be excluded on long averages. Moreover, our results are consistent with the diurnal cycle average of the two complete dry seasons of the GoAmazon project (2014 and 2015) described by Ghate and Kollias (2016). In future analyses, we intend to use a complete selection of events for the dry and wet seasons to improve our knowledge of morning transition and BL processes from the perspective of the Amazonian cloudy BL. In addition, a detailed analysis of large-eddy simulations on BL processes (e.g., river breeze), entrainment fluxes across the top of the convective BL, and turbulent kinetic energy budget on shallow and shallow-to-deep events is the subject of a future publication.

Data availability. The data used in this study are available in the ARM Climate Research Facility database for the GoAmazon 2014/5 experiment (https://www.arm.gov/research/campaigns/amf2014goamazon)

Author contributions. AH performed the analyses, and all the authors contribute to the writing of the manuscript.

Competing interests. The authors declare that they have no conflict of interest.

Acknowledgements. We acknowledge the data from the Atmospheric Radiation Measurement (ARM) Program sponsored by the U.S. Department of Energy, Office of Science, Office of Biological and Environmental Research, Climate and Environmental Sciences Division. AH acknowledges the Brazilian National Council for Scientific and Technological Development (CNPq) graduate fellowship (grant agreement number 140347/2019-4). The authors GF (process 307048/2018-7) and LATM (process 305301/2017-9) also thanks to CNPq for their Bolsa de Produtividade em Pesquisa. We also acknowledge FAPESP CHUVA Project Grant 2009/15235-8.

https://doi.org/10.5194/acp-2021-87
Preprint. Discussion started: 19 March 2021

Atmospheric Chemistry and Physics Discussions

Financial support. This work has received funding from the National Council for Scientific and Technological Development (grant agreement number 140347/2019-4) and from the EU FET VESTEC H2020 project, grant agreement number 800904.

https://doi.org/10.5194/acp-2021-87
Preprint. Discussion started: 19 March 2021

Atmospheric Chemistry and Physics Discussions

References

Atmospheric Radiation Measurement (ARM) user facility. 2014, updated hourly. Boundary-layer height data with CEIL (CEILPBLHT). 2014-01-01 to 2015-11-30, ARM Mobile Facility (MAO) Manacapuru, Amazonas, Brazil; AMF1 (M1). Compiled by V. Morris and Y. Shi. ARM Data Center. Data set accessed 2020-07-24, https://doi.org/http://dx.doi.org/10.5439/1095593, 2014a.

Atmospheric Radiation Measurement (ARM) user facility. 2014, updated hourly. Eddy Correlation Flux Measurement System (30ECOR). 2014-04-03 to 2015-12-01, ARM Mobile Facility (MAO) Manacapuru, Amazonas, Brazil; AMF1 (M1). Compiled by R. Sullivan, D. Cook and E. Keeler. ARM Data Center. Data set accessed 2020-07-24, https://doi.org/http://dx.doi.org/10.5439/1025039, 2014b.

Atmospheric Radiation Measurement (ARM) user facility. 2013, updated hourly. Radiative Flux Analysis (RADFLUX1LONG). 2013-12-23 to 2015-12-01, ARM Mobile Facility (MAO) Manacapuru, Amazonas, Brazil; AMF1 (M1). Compiled by C. Long, K. Gaustad and L. Riihimaki. ARM Data Center. Data set accessed 2019-04-04, https://doi.org/http://dx.doi.org/10.5439/1157585, 2014c.

Atmospheric Radiation Measurement (ARM): Surface Energy Balance System (SEBS). 2014-01-01 to 2015-12-01, ARM Mobile Facility (MAO) Manacapuru, Amazonas, Brazil; AMF1 (M1). Compiled by R. Sullivan, D. Cook and E. Keeler. Data set accessed 2020-11-14, https://doi.org/http://dx.doi.org/10.5439/1025274, 2014d.

Atmospheric Radiation Measurement (ARM) user facility. 2014, updated hourly. Mini Sound Detection and Ranging (SODAR). 2014-02-18 to 2015-12-01, ARM Mobile Facility (MAO) Manacapuru, Amazonas, Brazil; MAOS (S1). Compiled by R. Coulter, P. Muradyan and T. Martin. ARM Data Center. Data set accessed 2020-10-20, https://doi.org/http://dx.doi.org/10.5439/1150265, 2014e.

Atmospheric Radiation Measurement (ARM) user facility. 2014, updated hourly. Balloon-Borne Sounding System (SONDEWNPN). 2014-01-01 to 2015-12-01, ARM Mobile Facility (MAO) Manacapuru, Amazonas, Brazil; AMF1 (M1). Compiled by D. Holdridge, R. Coulter, J. Kyrouac and E. Keeler. ARM Data Center. Data set accessed 2020-07-09, https://doi.org/http://dx.doi.org/10.5439/1021460, 2014f.

Angevine, W. M., Baltink, H. K., and Bosveld, F. C.: Observations Of The Morning Transition Of The Convective Boundary Layer, Bound. Layer. Meteor., 101, 209–227, https://doi.org/10.1023/A:1019264716195, 2001.

Angevine, W. M., Edwards, J. M., Lothon, M., LeMone, M. A., and Osborne, S. R.: Transition Periods in the Diurnally-Varying Atmospheric Boundary Layer Over Land, Bound. Layer. Meteor., 177, 1–19, https://doi.org/10.1007/s10546-020-00515-y, 2020.

Betts, A., Fisch, G., Von Randow, C., Silva Dias, M., Cohen, J., Da Silva, R., and Fitzjarrald, D.: The Amazonian boundary layer and mesoscale circulations, pp. 163–181, American Geophysical Union (AGU), https://doi.org/10.1029/2008GM000720, 2009.

Betts, A. K. and Viterbo, P.: Land-surface, boundary layer, and cloud-field coupling over the southwestern Amazon in ERA-40, J. Geophys. Res. Atmos., 110, https://doi.org/10.1029/2004JD005702, 2005.

Biscaro, T. S., Machado, L. A., Giangrande, S. E., and Jensen, M. P.: What Drives Daily Precipitation Over Central Amazon? Differences Observed Between Wet and Dry Seasons, Atmos. Chem. Phys. Discuss., pp. 1–25, https://doi.org/10.5194/acp-2020-1098, 2020.

Carneiro, R. G. and Fisch, G.: Observational analysis of the daily cycle of the planetary boundary layer in the central Amazon during a non-El Niño year and El Niño year (GoAmazon project 2014/5), Atmos. Chem. Phys., 20, 5547–5558, https://doi.org/10.5194/acp-20-5547-2020, 2020.

Carneiro, R. G., Fisch, G., Borges, C. K., and Henkes, A.: Erosion of the nocturnal boundary layer in the central Amazon during the dry season, Acta Amaz., 50, 80–89, https://doi.org/10.1590/1809-4392201804453, 2020.

Chaboureau, J.-P., Guichard, F., Redelsperger, J.-L., and Lafore, J.-P.: The role of stability and moisture in the diurnal cycle of convection over land, Q. J. Roy. Meteorol. Soc., 130, 3105–3117, https://doi.org/10.1256/qj.03.132, 2004.

https://doi.org/10.5194/acp-2021-87
Preprint. Discussion started: 19 March 2021

Atmospheric Chemistry and Physics Discussions

Chakraborty, S., Schiro, K. A., Fu, R., and Neelin, J. D.: On the role of aerosols, humidity, and vertical wind shear in the transition of shallow-to-deep convection at the Green Ocean Amazon 2014/5 site, Atmos. Chem. Phys., 18, 11 135–11 148, https://doi.org/10.5194/acp-18-11135-2018, 2018.

Feng, Z. and Giangrande, S.: Merged RWP-WACR-ARSCL Cloud Mask and Cloud Type, https://doi.org/10.5439/1462693, 2018.

Fisch, G., Tota, J., Machado, L. A. T., Silva Dias, M. A. F., da F. Lyra, R. F., Nobre, C. A., Dolman, A. J., and Gash, J. H. C.: The convective boundary layer over pasture and forest in Amazonia, Theor. Appl. Climatol., 78, 47–59, https://doi.org/10.1007/s00704-004-0043-x, 2004.

Fitzjarrald, D. R., Sakai, R. K., Moraes, O. L. L., Cosme de Oliveira, R., Acevedo, O. C., Czikowsky, M. J., and Beldini, T.: Spatial and temporal rainfall variability near the Amazon-Tapajós confluence, J. Geophys. Res. Biogeosc., 113, https://doi.org/10.1029/2007JG000596, 2008.

Ghate, V. P. and Kollias, P.: On the Controls of Daytime Precipitation in the Amazonian Dry Season, J. Hydrometeorol., 17, 3079–3097, https://doi.org/10.1175/JHM-D-16-0101.1, 2016.

Giangrande, S. E., Feng, Z., Jensen, M. P., Comstock, J. M., Johnson, K. L., Toto, T., Wang, M., Burleyson, C., Bharadwaj, N., Mei, F., Machado, L. A. T., Manzi, A. O., Xie, S., Tang, S., Silva Dias, M. A. F., de Souza, R. A. F., Schumacher, C., and Martin, S. T.: Cloud characteristics, thermodynamic controls and radiative impacts during the Observations and Modeling of the Green Ocean Amazon (GoAmazon2014/5) experiment, Atmos. Chem. Phys., 17, 14 519–14 541, https://doi.org/10.5194/acp-17-14519-2017, 2017.

Giangrande, S. E., Wang, D., and Mechem, D. B.: Cloud regimes over the Amazon Basin: perspectives from the GoAmazon2014/5 campaign, Atmos. Chem. Phys., 20, 7489–7507, https://doi.org/10.5194/acp-20-7489-2020, 2020.

Khairoutdinov, M. and Randall, D.: High-resolution simulation of shallow-to-deep convection transition over land, J. Atmos. Sci., 63, 3421–3436, https://doi.org/10.1175/JAS3810.1, 2006.

Machado, L. A. T., Calheiros, A. J. P., Biscaro, T., Giangrande, S., Silva Dias, M. A. F., Cecchini, M. A., Albrecht, R., Andreae, M. O., Araujo, W. F., Artaxo, P., Borrmann, S., Braga, R., Burleyson, C., Eichholz, C. W., Fan, J., Feng, Z., Fisch, G. F., Jensen, M. P., Martin, S. T., Pöschl, U., Pöhlker, C., Pöhlker, M. L., Ribaud, J.-F., Rosenfeld, D., Saraiva, J. M. B., Schumacher, C., Thalman, R., Walter, D., and Wendisch, M.: Overview: Precipitation characteristics and sensitivities to environmental conditions during GoAmazon2014/5 and ACRIDICON-CHUVA, Atmos. Chem. Phys., 18, 6461–6482, https://doi.org/10.5194/acp-18-6461-2018, 2018.

Mahrt, L. and Vickers, D.: Contrasting vertical structures of nocturnal boundary layers, Bound. Layer. Meteor., 105, 351–363, https://doi.org/10.1023/A%3A1019964720989, 2002.

Martin, S. T., Artaxo, P., Machado, L. A. T., Manzi, A. O., Souza, R. A. F., Schumacher, C., Wang, J., Andreae, M. O., Barbosa, H. M. J., Fan, J., Fisch, G., Goldstein, A. H., Guenther, A., Jimenez, J. L., Pöschl, U., Silva Dias, M. A., Smith, J. N., and Wendisch, M.: Introduction: Observations and Modeling of the Green Ocean Amazon (GoAmazon2014/5), Atmos. Chem. Phys., 16, 4785–4797, https://doi.org/10.5194/acp-16-4785-2016, 2016.

Martin, S. T., Artaxo, P., Machado, L., Manzi, A. O., Souza, R. A. F., Schumacher, C., Wang, J., Biscaro, T., Brito, J., Calheiros, A., Jardine, K., Medeiros, A., Portela, B., de Sá, S. S., Adachi, K., Aiken, A. C., Albrecht, R., Alexander, L., Andreae, M. O., Barbosa, H. M. J., Buseck, P., Chand, D., Comstock, J. M., Day, D. A., Dubey, M., Fan, J., Fast, J., Fisch, G., Fortner, E., Giangrande, S., Gilles, M., Goldstein, A. H., Guenther, A., Hubbe, J., Jensen, M., Jimenez, J. L., Keutsch, F. N., Kim, S., Kuang, C., Laskin, A., McKinney, K., Mei, F., Miller, M., Nascimento, R., Pauliquevis, T., Pekour, M., Peres, J., Petäjä, T., Pöhlker, C., Pöschl, U., Rizzo, L., Schmid, B., Shilling, J. E., Dias, M. A. S., Smith, J. N., Tomlinson, J. M., Tóta, J., and Wendisch, M.: The Green Ocean Amazon Experiment

(GoAmazon2014/5) Observes Pollution Affecting Gases, Aerosols, Clouds, and Rainfall over the Rain Forest, Bull. Amer. Meteo. Soc., 98, 981–997, https://doi.org/10.1175/BAMS-D-15-00221.1, 2017.

Mather, J. H. and Voyles, J. W.: The Arm Climate Research Facility: A Review of Structure and Capabilities, Bull. Amer. Meteo. Soc., 94, 377–392, https://doi.org/10.1175/BAMS-D-11-00218.1, 2013.

Oliveira, M. I., Acevedo, O. C., Sörgel, M., Nascimento, E. L., Manzi, A. O., Oliveira, P. E., Brondani, D. V., Tsokankunku, A., and Andreae, M. O.: Planetary boundary layer evolution over the Amazon rainforest in episodes of deep moist convection at the Amazon Tall Tower Observatory, Atmos. Chem. Phys., 20, 15–27, https://doi.org/10.5194/acp-20-15-2020, 2020.

Pielke Sr, R. A.: Influence of the spatial distribution of vegetation and soils on the prediction of cumulus convective rainfall, Rev. Geophys., 39, 151–177, https://doi.org/10.1029/1999RG000072, 2001.

Schiro, K. A. and Neelin, J. D.: Tropical continental downdraft characteristics: mesoscale systems versus unorganized convection, Atmos. Chem. Phys., 18, 1997—-2010, https://doi.org/10.5194/acp-18-1997-2018, 2018.

Stull, R. B.: An Introduction to Boundary Layer Meteorology, Springer, Dordrecht, https://doi.org/10.1007/978-94-009-3027-8, 1988.

Tang, S., Xie, S., Zhang, Y., Zhang, M., Schumacher, C., Upton, H., Jensen, M. P., Johnson, K. L., Wang, M., Ahlgrimm, M., Feng, Z., Minnis, P., and Thieman, M.: Large-scale vertical velocity, diabatic heating and drying profiles associated with seasonal and diurnal variations of convective systems observed in the GoAmazon2014/5 experiment, Atmos. Chem. Phys., 16, 14 249–14 264, https://doi.org/10.5194/acp-16-14249-2016, 2016.

Tennekes, H.: A Model for the Dynamics of the Inversion Above a Convective Boundary Layer, J. Atmos. Sci., 30, 558–567, https://doi.org/10.1175/1520-0469(1973)030<0558:AMFTDO>2.0.CO;2, 1973.

Wang, D., Giangrande, S. E., Bartholomew, M. J., Hardin, J., Feng, Z., Thalman, R., and Machado, L. A.: The Green Ocean: precipitation insights from the GoAmazon2014/5 experiment, Atmos. Chem. Phys., 18, 2018.

Wilson, J. W., Crook, N. A., Mueller, C. K., Sun, J., and Dixon, M.: Nowcasting thunderstorms: A status report, Bull. Amer. Meteo. Soc., 79, 2079–2100, https://doi.org/10.1175/1520-0477(1998)079%3C2079:NTASR%3E2.0.CO;2, 1998.

Wu, C.-M., Stevens, B., and Arakawa, A.: What controls the transition from shallow to deep convection?, J. Atmos. Sci., 66, 1793–1806, https://doi.org/10.1175/2008JAS2945.1, 2009.

Zhang, Y. and Klein, S. A.: Mechanisms Affecting the Transition from Shallow to Deep Convection over Land: Inferences from Observations of the Diurnal Cycle Collected at the ARM Southern Great Plains Site, J. Atmos. Sci., 67, 2943–2959, https://doi.org/10.1175/2010JAS3366.1, 2010.

Zhuang, Y., Fu, R., Marengo, J. A., and Wang, H.: Seasonal variation of shallow-to-deep convection transition and its link to the environmental conditions over the Central Amazon, J. Geophys. Res. Atmos., 122, 2649–2666, https://doi.org/10.1002/2016JD025993, 2017.

https://doi.org/10.5194/acp-2021-87
Preprint. Discussion started: 19 March 2021

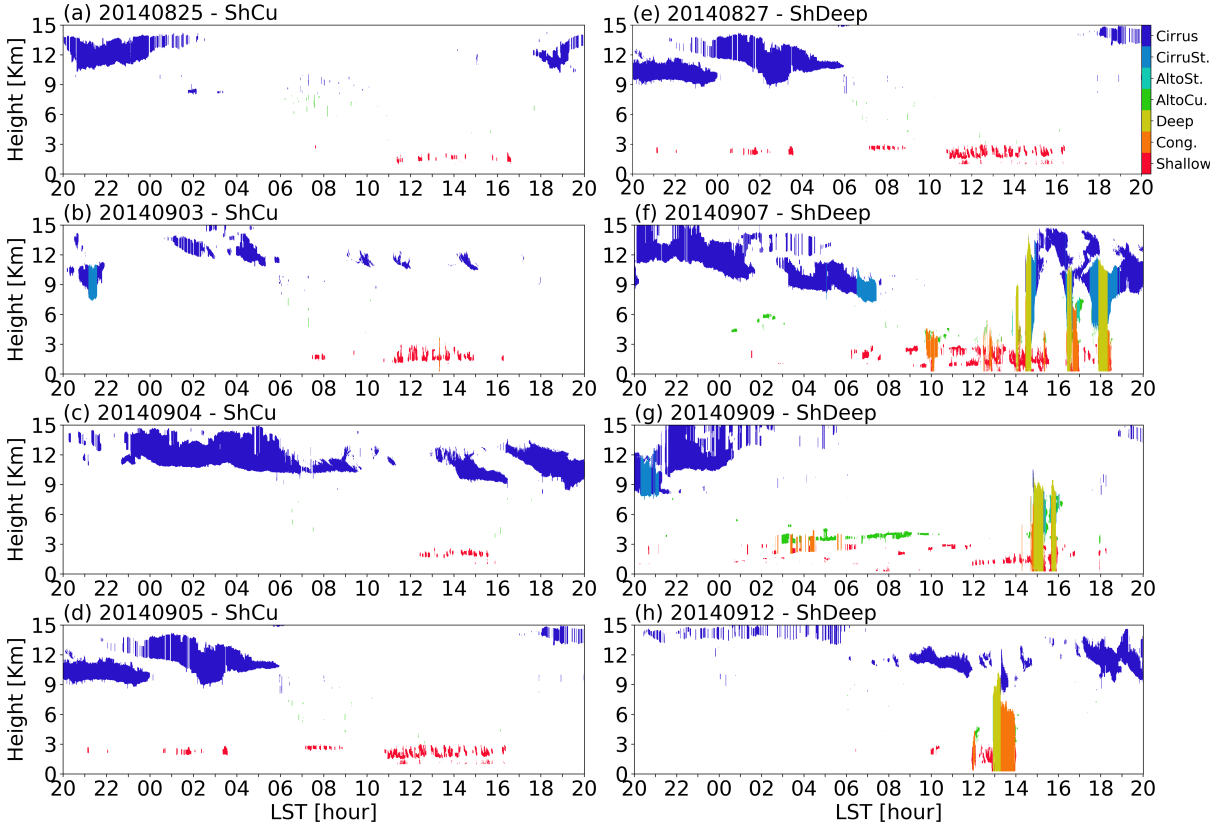

Figure 1. Cloud-type classification from the ARSCL product for corresponding dates of **(a–d)** shallow convective (ShCu) days on the left-hand panels and **(e–h)** shallow-to-deep convective (ShDeep) days on right-hand panels.

https://doi.org/10.5194/acp-2021-87
Preprint. Discussion started: 19 March 2021

Atmospheric Chemistry and Physics Discussions

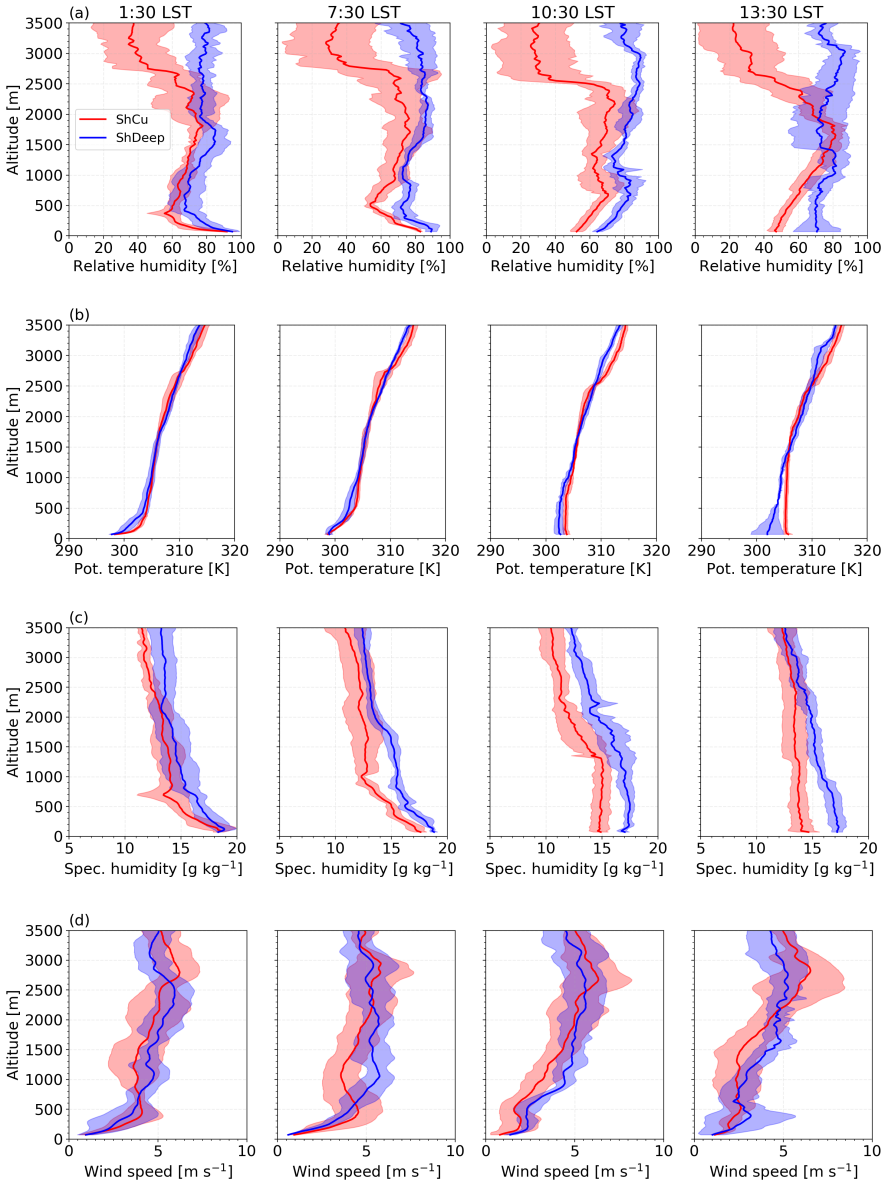

Figure 2. Vertical profiles between 50 and 3500 m of **(a)** relative humidity, **(b)** potential temperature, **(c)** specific humidity, and **(d)** wind speed from radiosondes launched at the T3 site (from left to right) at 1:30, 7:30, 10:30, and 13:30 LST. The mean (bold lines) and the standard deviation (shadings) are shown for shallow convective (ShCu, red) and shallow-to-deep convective (ShDeep, blue) days.

https://doi.org/10.5194/acp-2021-87
Preprint. Discussion started: 19 March 2021

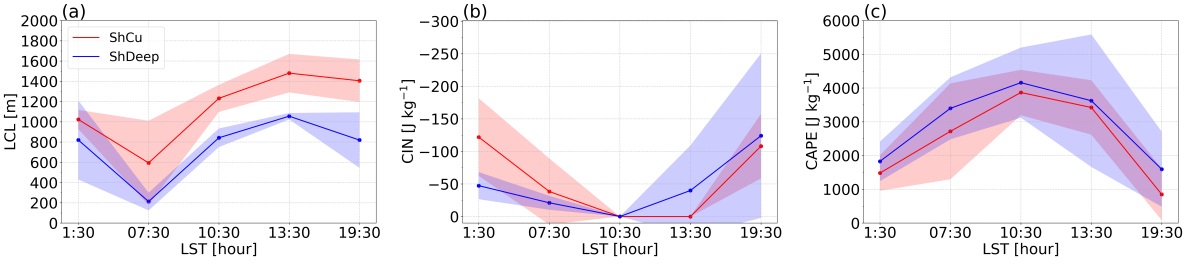

Figure 3. Time evolution of **(a)** lifting condensation level (LCL), **(b)** convective inhibition (CIN) and **(c)** convective available potential energy (CAPE) derived from radiosondes. The mean (bold lines) and the standard deviation (shadings) are shown for shallow convective (ShCu, red) and shallow-to-deep convective (ShDeep, blue) days.

https://doi.org/10.5194/acp-2021-87
Preprint. Discussion started: 19 March 2021

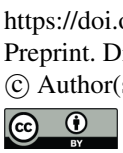

Atmospheric Chemistry and Physics Discussions

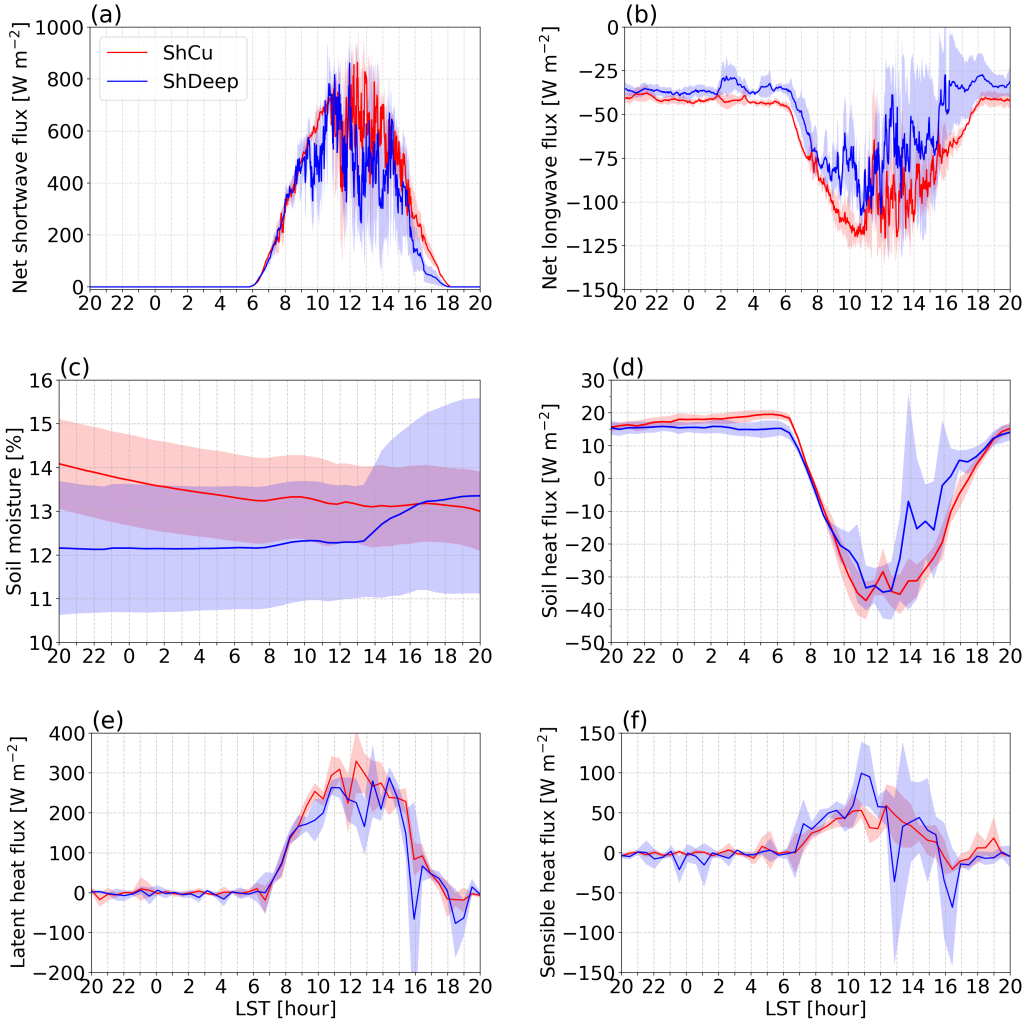

Figure 4. Time evolution of **(a)** net shortwave radiative flux, **(b)** net longwave radiative flux, **(c)** soil moisture at superficial layer, **(d)** soil heat flux, **(e)** latent heat flux and **(f)** sensible heat flux at the surface. The mean (bold lines) and the standard deviation (shadings) are shown for shallow convective (ShCu, red) and shallow-to-deep convective (ShDeep, blue) days.

https://doi.org/10.5194/acp-2021-87
Preprint. Discussion started: 19 March 2021

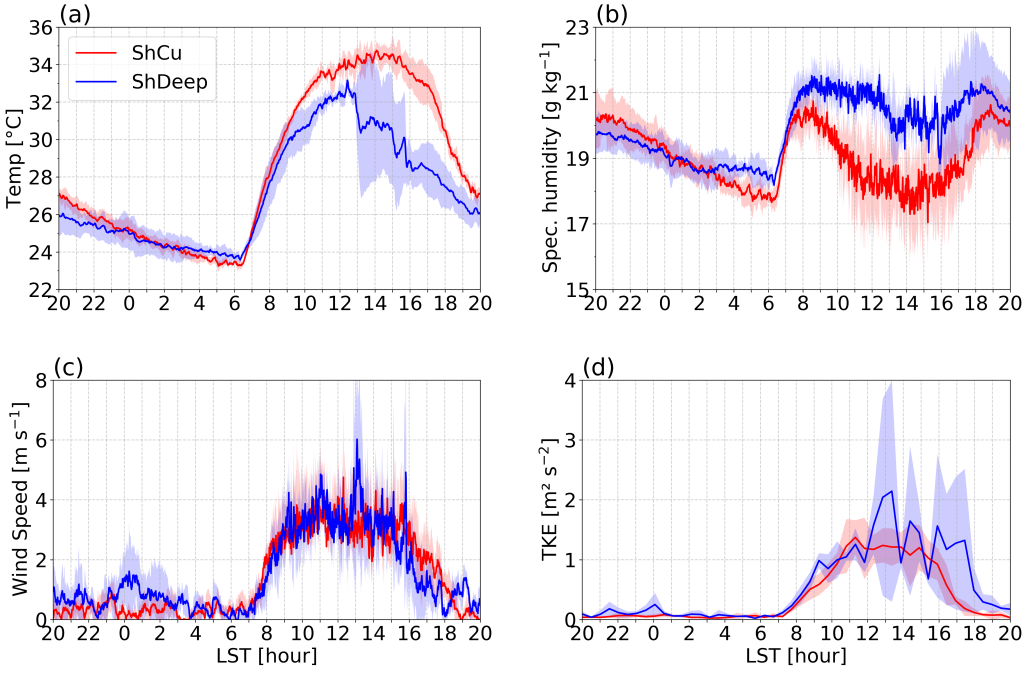

Figure 5. As in Fig. 4 but for **(a)** surface air temperature, **(b)** specific humidity, (**c**) wind speed estimated by surface meteorological system, and **(d)** turbulent kinetic energy estimated by ECOR.

https://doi.org/10.5194/acp-2021-87
Preprint. Discussion started: 19 March 2021

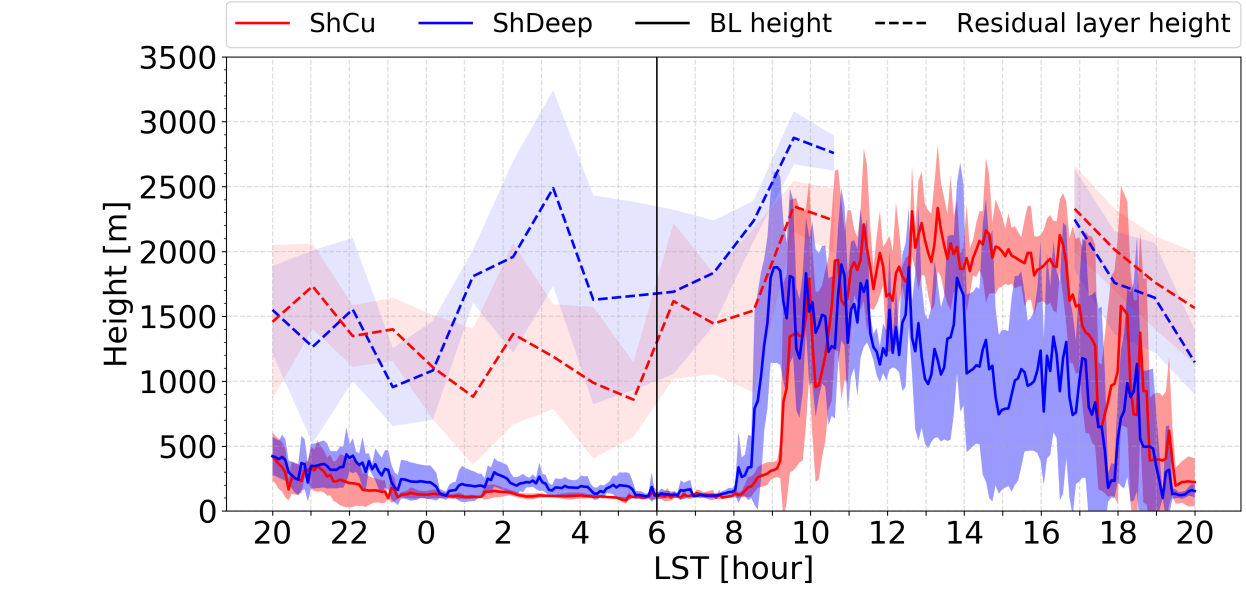

Figure 6. As in Fig. 4 but for the height of the BL (solid) and the residual boundary layer height (dashed).

https://doi.org/10.5194/acp-2021-87
Preprint. Discussion started: 19 March 2021

Atmospheric Chemistry and Physics Discussions

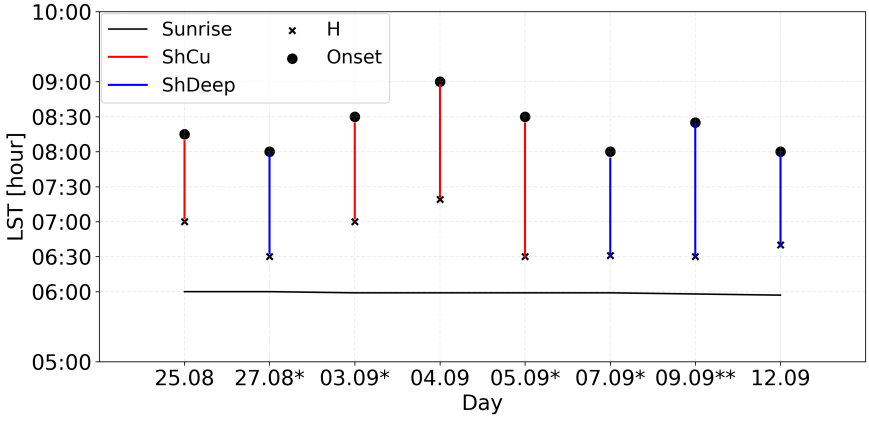

Figure 7. Times of sunrise (line), sensible heat flux crossover (H, "x"), and onset of convective BL estimated by ceilometer (Onset, circles) corresponding to eight morning transition days. The red and blue lines correspond to shallow convective (ShCu) and shallow-to-deep convective (ShDeep) days, respectively. The days with shallow cloud influence is marked as asterisk and day AltoCumulus cloud influence is marked as double asterisk.

https://doi.org/10.5194/acp-2021-87
Preprint. Discussion started: 19 March 2021

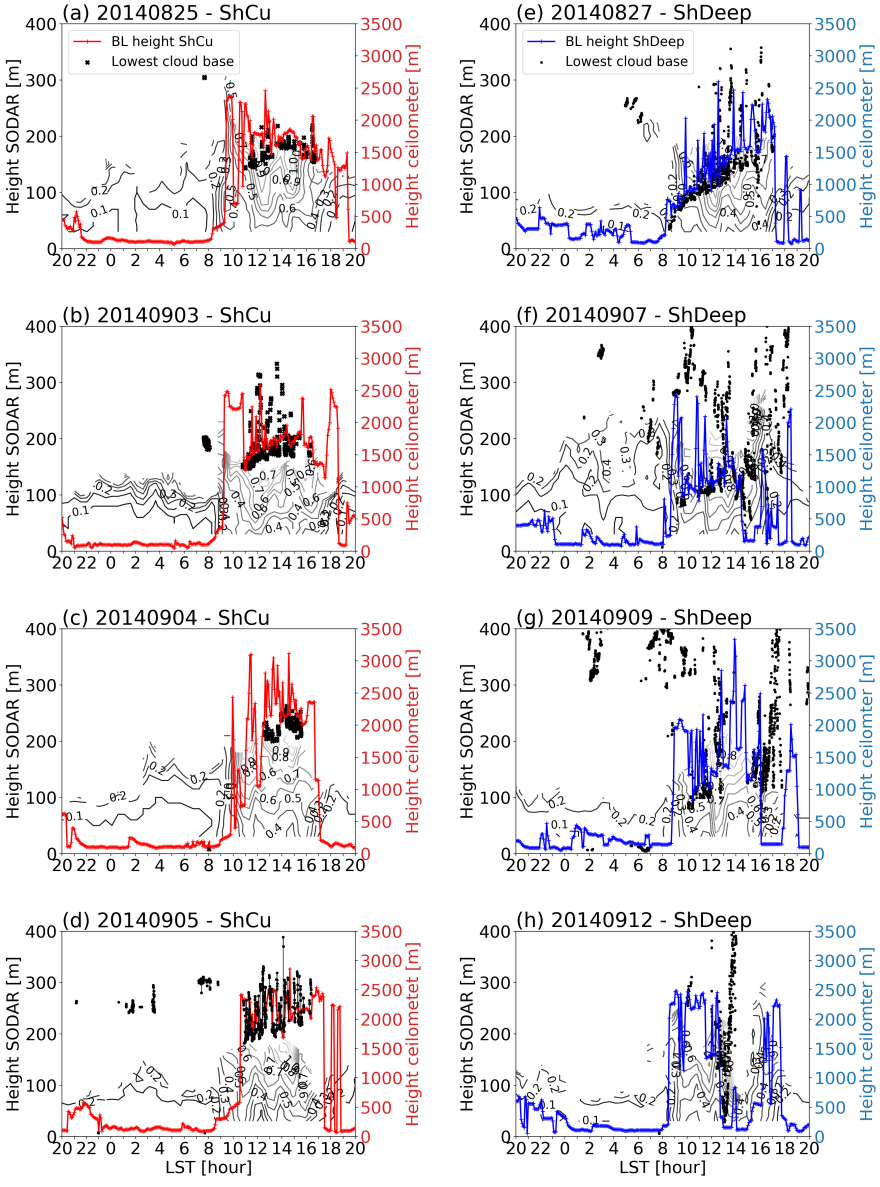

Figure 8. As in Fig. 4 but for the height of the BL on **(a–d)** ShCu days and **(e–h)** ShDeep days. The contour shows the standard deviation of vertical velocity estimated by SODAR. The contour starts at 0.1 and increments every 0.1 m s^{-1}.

https://doi.org/10.5194/acp-2021-87
Preprint. Discussion started: 19 March 2021

Atmospheric Chemistry and Physics Discussions

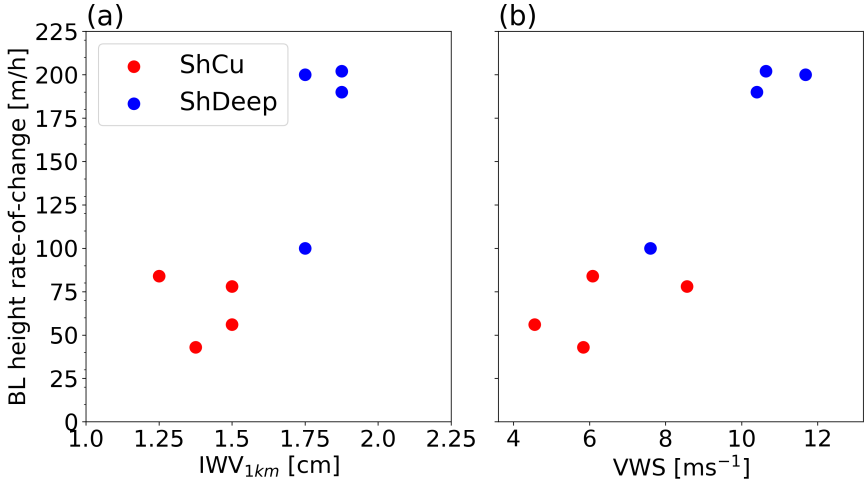

Figure 9. Scatterplots of the BL height rate-of-change versus **(a)** integrated water vapor from 50 to 1000 m (IWV_{1km}) and **(b)** vertical wind shear (VWS) between 50 m and 1000 m for shallow-to-deep convective (ShDeep, blue circles) and shallow convective (ShCu, red circles) days.

https://doi.org/10.5194/acp-2021-87
Preprint. Discussion started: 19 March 2021

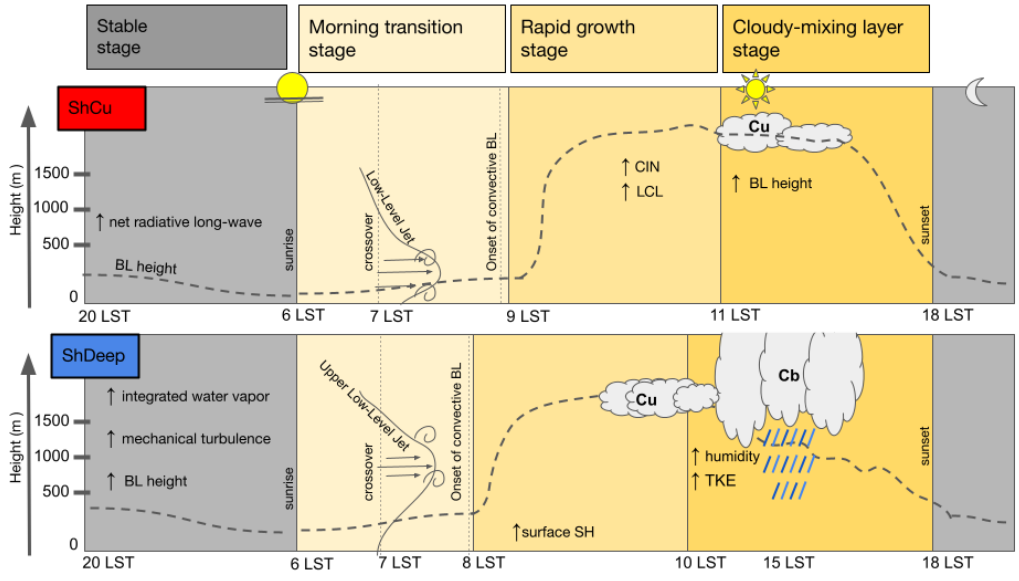

Figure 10. Conceptual model of BL processes on ShCu (top) and ShDeep days (bottom) illustrating the cloudy-BL stages during the dry season over Central Amazon. The BL height is represented by the dashed curves on both regimes. BL, SH, CIN, LCL, and TKE stand for the boundary layer, sensible heat flux, convective inhibition, lifting condensation level, and turbulent kinetic energy respectively.

https://doi.org/10.5194/acp-2021-87
Preprint. Discussion started: 19 March 2021

Atmospheric Chemistry and Physics Discussions

Table 1. List of non-transition shallow convective (ShCu) and transitions shallow-to-deep convective (ShDeep) days selected during the IOP2.

Day	Date	Convective regime	Event Description	Precipitation rate [mm h^{-1}]
1	2014/08/25	ShCu	Scattered shallow cumulus convective cells	0
2	2014/08/27	ShDeep	Scattered shallow-to-deep convective cells	4.0
3	2014/09/03	ShCu	Scattered shallow cumulus convective cells	0
4	2014/09/04	ShCu	Scattered shallow cumulus convective cells	0
5	2014/09/05	ShCu	Scattered shallow cumulus convective cells	0
6	2014/09/07	ShDeep	Scattered shallow-to-deep convective cells	3.3
7	2014/09/09	ShDeep	Scattered shallow-to-deep convective cells	3.4
8	2014/09/12	ShDeep	Scattered shallow-to-deep convective cells	4.7

https://doi.org/10.5194/acp-2021-87
Preprint. Discussion started: 19 March 2021

Atmospheric Chemistry and Physics Discussions

Table 2. Meteorological parameters for each case study day during the morning-transition stage. Reference time of first positive significant value of sensible heat flux (Crossover); Time to erode the nocturnal BL relative to sunrise (Onset CBL); Change in BL height during morning transition stage (rates-of-change); The 50 m value of specific humidity (q_{surf}); Integrated Water Vapor from 50 to 1000 m (IWV_{1km}); total column IWV of are reported in parentheses (IWV_T), Vertical Wind Shear between 1000 and 50 m (VWS_{1km}); Low-level jet maximum (LLJ) and in parentheses are also reported the respective maximum heights. The q_{surf}, IVW, VWS, LLJ are computed using the 07:30 LST radiosoundings. Days with cloud influence during the morning transition stage are marked with an asterisk.

Event	Date	crossover time [h](value)	Onset CBL [h]	rates-of-change [m h^{-1}]	q_{surf} [g kg^{-1}]	IWV [cm]	VWS_{1km} [m s^{-1}]	LLJ [m s^{-1}](height)
1	2014/08/25	07:30 (20.0 Wm^{-2})	2:30	84.0	19.6	1.2 (4.6)	5.1	11.3 (330 m)
2*	2014/08/27	06:30 (2.0 Wm^{-2})	2:15	190.0	19.6	1.7 (4.9)	10.5	15.0(1350 m)
3*	2014/09/03	06:30 (3.0 Wm^{-2})	3:00	78.0	18.7	1.5 (4.4)	8.2	13.7 (630 m)
4	2014/09/04	07:30 (17.0 Wm^{-2})	2:30	43.0	20.0	1.4 (3.4)	4.8	8.6 (350 m)
5*	2014/09/05	07:00 (0.1 Wm^{-2})	2:30	56.0	20.4	1.3 (3.6)	3.2	6.6 (610 m)
6*	2014/09/07	07:00 (23.0 Wm^{-2})	2:10	202.0	20.5	1.7 (5.1)	10.8	12.7(890 m)
7*	2014/09/09	07:00 (44.0 Wm^{-2})	2:30	200.0	20.1	1.6 (5.1)	12.1	13.2(1010 m)
8	2014/09/12	06:30 (8.0 Wm^{-2})	2:00	100.0	21.0	1.6 (4.6)	7.0	non-LLJ

non LLJ = no LLJ is detected